ELSEVIER

Catalysis Today 63 (2000) 479–487

CATALYSIS TODAY

www.elsevier.com/locate/cattod

Kinetics of internal steam reforming of methane on Ni/YSZ-based anodes for solid oxide fuel cells

Khaliq Ahmed*, Karl Foger

Ceramic Fuel Cells Ltd., 170 Browns Road, Noble Park, Vic. 3174, Australia

Abstract

The kinetics of steam reforming of methane was determined on a Ni-YSZ anode, which we refer to as anode 'A' and on a Ni-YSZ anode modified by the addition of a basic compound, which we refer to as anode 'B'. A salient feature of our work is that the data were collected on 50 μm thick anodes screen-printed on 110 μm thick YSZ electrolytes and the experiments were carried out in a fuel cell configuration. Orders in methane and steam were both higher on the modified Ni-YSZ anode. Activation energy was also higher on this anode suggesting different nature of sites in the two anodes. In the present study we have attempted to generate kinetic data at steam/carbon ratios which are economically attractive for fuel cell operation.

Keywords: Kinetics; Methane; Ni-YSZ anode

1. Introduction

Internal steam reforming of methane is preferred by SOFC developers as it has several advantages:

1. The heat released from the fuel cell reaction, which is mainly due to energy losses and heat production caused by polarization and ohmic losses of the fuel cell, can provide the endothermic heat of the steam reforming reaction. Heat consumption by the steam reforming reaction is about half of the heat production rate in the stack under typical operating conditions.
2. Part of the steam required for the reforming reaction can be obtained from the steam generated by the fuel cell reaction. Therefore less steam is required; this is even more so with anode off-gas recycle.
3. The reforming reaction can proceed beyond the thermodynamic equilibrium because of the continuing consumption of hydrogen by the fuel cell reaction.
4. The requirement of cell cooling which is usually achieved by flowing excess air through the cathode is much smaller. Under typical operating conditions, the cooling load is reduced by 40–50%.
5. A more evenly distributed supply of hydrogen is achieved, which can potentially lead to a more even temperature distribution in the stack.
6. With no separate external reformer, significant reduction in capital investment and operating costs is achieved.
7. Has the potential to offer faster response to load variations.

This approach, however, may pose some of the following problems in the stack:

1. There is a risk of carbon formation on current Ni-based SOFC anodes. High steam/carbon ratios typically used in conventional steam reformers to suppress carbon formation is unattractive for fuel cells as it lowers the electrical efficiency of the fuel

---

* Corresponding author.

PII: S0920-5861(00)00494-6

cell by steam dilution of the fuel. In addition, there are concerns related to Ni oxidation and redistribution, particularly at high fuel utilization. Hence, there is a search for advanced catalysts which will allow internal reforming at low steam carbon ratios.
2. Excessively large temperature gradients can develop across the cell and interconnect plate due to endothermal cooling. Reforming is usually complete within a small distance on the anode. This leads to a strong cooling effect near the fuel-inlet zone resulting in large temperature gradients.

There are two approaches to reducing the extent of these problems. One is partial pre-reforming of natural gas. With increased levels of pre-reforming, however, some of the advantages of full internal reforming of methane is sacrificed. The degree of pre-reforming needs to be optimized from a consideration of the advantages and disadvantages of internal reforming. A second approach is to extend the reaction zone on the anode by reducing the rate of reforming on the anode, usually achieved by partial poisoning of active sites using appropriate modifications or promoters. Again, with this approach too, some of the advantages of internal reforming are lost at least partially; the anode formulation needs to be optimized. Experimental data using a combination of the two approaches were reported earlier [1].

Information on the effects of internal reforming on stack performance with different stack manifold design, anode-recycle and load changes can be obtained by mathematical modeling of the stack. In order to develop an effective model, detailed knowledge of the kinetics of the reforming reaction is required.

Nickel–zirconia based anodes are used by many SOFC developers for internal reforming of methane in SOFC stacks. There have been some papers published in recent years with information on the kinetics of steam reforming of nickel-based anode materials [1–11]. There are two important observations to be made from a review of the literature. Firstly, there is some disagreement with regard to the dependency of methane reforming rate on the partial pressures of the reactants, particularly, steam. Secondly, the reported activation energies range from 60 to 230 kJ/mol. A major criticism of the work on internal reforming kinetics, reported in the literature, is that these have been carried out using catalyst forms that are not used in solid oxide fuel cells. SOFC anode manufacturing processes are different from the conventional catalyst preparation techniques. Therefore anode formulations prepared by conventional methods and in conventional forms bear little relevance to the SOFC anodes which may have different pore structure and nickel particle size. A salient feature of our work is that the data were collected on 50 μm thick anodes screen-printed on 100 μm zirconia electrolytes and the experiments were carried out in a fuel cell configuration. The fuel cell reactor was operated in the differential mode with conversions ranging from 10 to 25%.

In the present work we report kinetic data during internal reforming of methane on two anodes:

1. Ni-YSZ anode;
2. Ni-YSZ anode modified by the addition of a basic compound.

2. Experimental

2.1. Experimental setup

The experimental setup is a single-cell SOFC stack which uses 50 mm × 50 mm PEN. It is composed of three sections.

2.1.1. Feed

The feed section contains gas supply lines for CO, H_2, CO_2, CH_4 and Ar the latter being used as a diluent. The gases flow through their respective mass flow controllers and are then mixed in a mixing chamber. Steam is generated by de-ionized water in a humidifier whose temperature and level are controlled. The fuel-inlet pipe from the humidifier to the reaction section base is heated by heating tape and kept at a temperature of 150°C.

2.1.2. Reactor

The reaction chamber with its inlet and outlet pipes is made of alumina. This is to avoid carbon formation as well as to prevent the reactants from reacting prior to reaching the anode catalyst. The reactor with its inlet and outlet pipes are enclosed within a vertical split-tubular furnace. The exhaust gas from the reactor is passed through a condenser where the unreacted steam is condensed and separated. The dry gas from the condenser is passed through a back-pressure regulator to allow a stream of the exhaust gas to go to the analysis section.

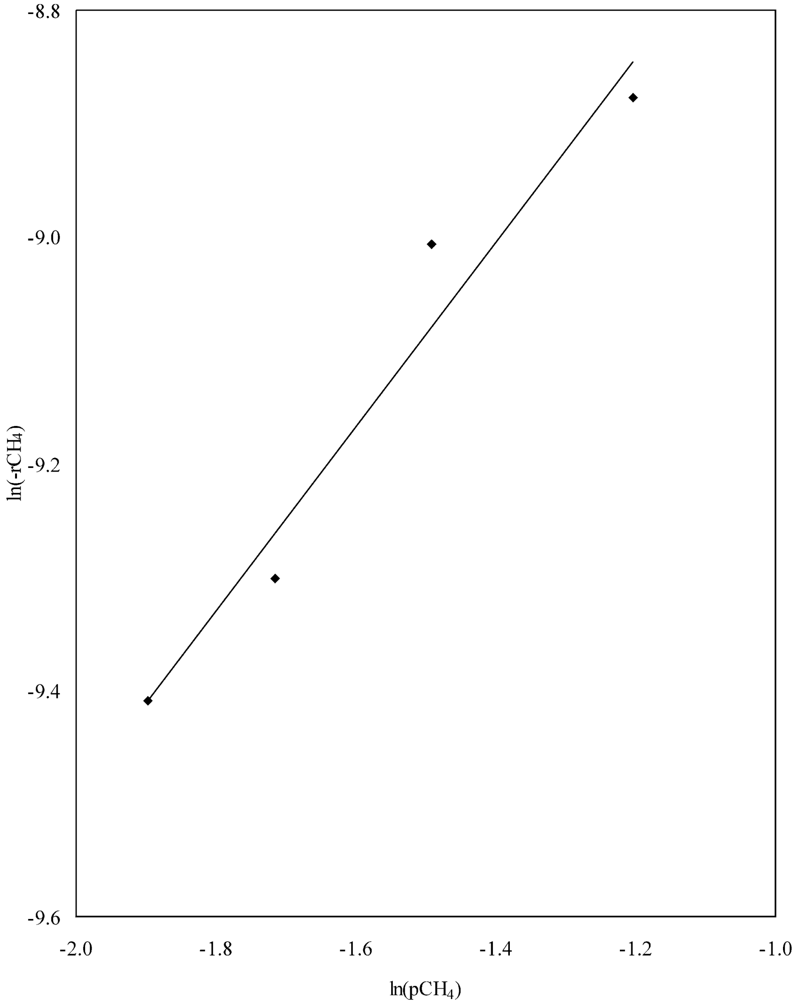

Fig. 1. Rate of reforming vs. p_{CH_4} on anode ‘A’ (880°C, $S/C = 1.5$ to 3.0, $p_{H_2O} = 0.45$ bar).

2.1.3. Analysis

The analysis section consists of a gas chromatograph where the gases CH_4, CO, CO_2 and H_2 are separated in a capillary column and analyzed by a thermal conductivity detector. The analysis method was calibrated using a gas mixture of known composition containing the gases CH_4, CO, CO_2 and H_2.

2.2. Materials

All the gases were supplied by BOC and were of 99.5+% purity. The GC carrier gas had a purity of 99.995%. The catalyst anodes used in the present investigation were prepared in our laboratories.

2.3. Procedure

A glass seal supported in gasket form was placed in the fuel cell manifold. The substrate containing the screen-printed test anode and LSM cathode was placed over it. The cathode reaction chamber with its air inlet tube was placed over the PEN. During heating up to the reaction temperature, the glass melted and formed a seal in the anode chamber. The anode was reduced in

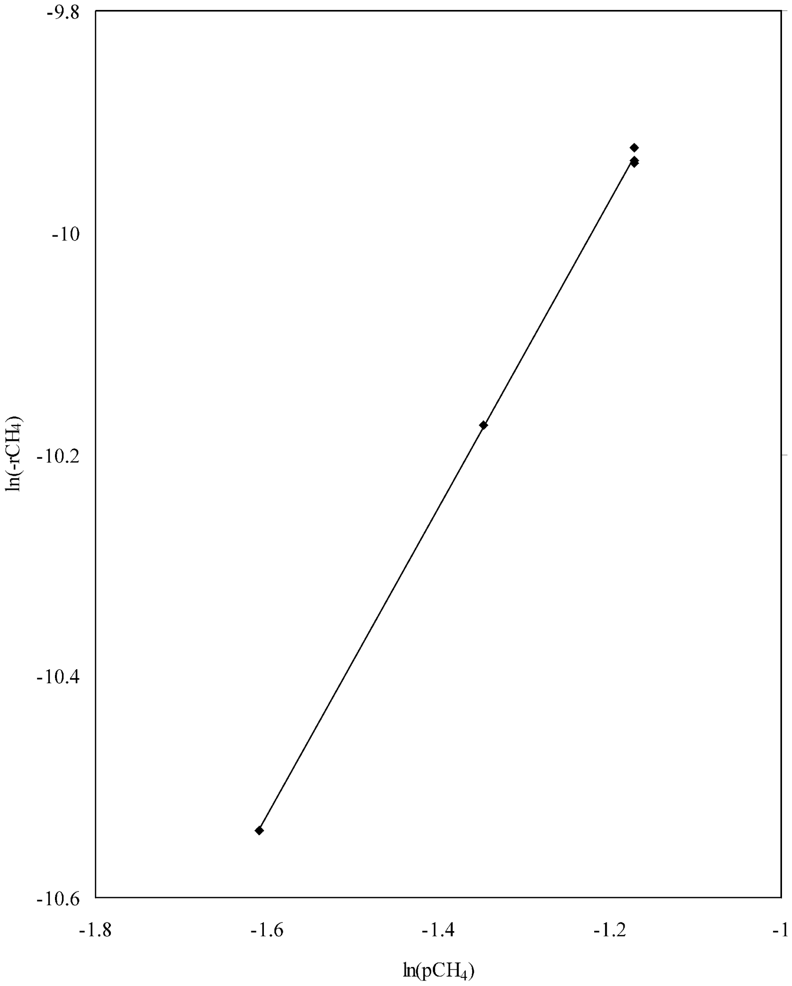

Fig. 2. Rate of reforming vs. p_{CH_4} on anode ‘B’ (895°C, $S/C = 1.7$ to 2.6, $p_{H_2O} = 0.52$ bar).

hydrogen flow for ∼2 h at 900°C before commencing the steam reforming experiments. Air was flown over the cathode at 1.5 l/min. Stability of open-circuit voltage and exit-gas composition were monitored for ∼2 h before collecting kinetic data under each test condition.

3. Results and discussion

A temperature range 854–907°C was covered in the experiments with anode ‘A’. Steam/carbon ratio ranged from 1.53 to 2.5; p_{CH_4} was 0.15–0.3 bar and p_{H_2O} was 0.23–0.45 bar.

For anode ‘B’, the temperature range was 838–922°C. Steam/carbon ratio was 1.4–3.0; p_{CH_4} was 0.2–0.35 bar and p_{H_2O} was 0.28–0.60 bar.

Generation of steam reforming kinetic data on Ni-based anodes is rendered difficult because of the fact that nickel catalysts are particularly prone to carbon deposition when the steam/carbon ratios are relatively low (<3). A high steam/carbon ratio is required to prevent carbon deposition unless the catalyst is modified by the addition of certain compounds that impart resistance to carbon formation. Our own work on unmodified Ni-YSZ cermet anodes have shown that steam/carbon ratios of 3–5 are generally required to avoid carbon deposition. However, with modified

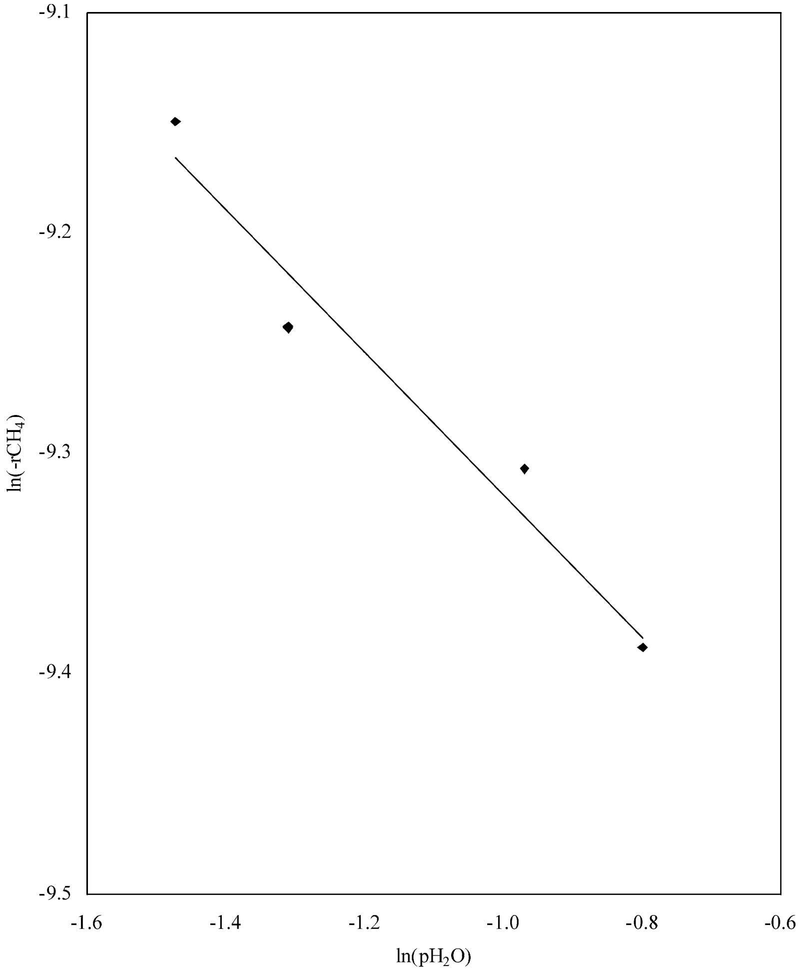

Fig. 3. Rate of reforming vs. p_{H_2O} on anode ‘A’ (880°C, S/C = 1.5 to 3.0, $p_{CH_4} = 0.15$ bar).

Ni-based anodes we have successfully operated at much lower steam/carbon ratios as reported earlier [1].

In the present study, we have attempted to generate kinetic data at steam/carbon ratios which are economically attractive for fuel cell operation. Our modified anode (anode ‘B’) is robust enough to give protection against carbon formation at the low steam carbon ratios of 1.4–3.0 employed in the present study. Gas composition and open-circuit voltage were essentially stable during the measurements. For both anodes the accuracy of data is not better than ±5% as this is the accuracy of the gas mixture used for calibration of the gas chromatograph. Other uncertainties in measurements (e.g. gas flow rate, steam content, temperature and pressure) may well increase the errors to ±10%. Nevertheless, data presented below show quite acceptable goodness of fit for the plots of order dependencies and activation energy on both anodes.

The rate expression is assumed to be of the following form:

$$-r_{CH_4} = kp_{CH_4}{}^{\alpha} p_{H_2O}{}^{\beta} \exp\left(\frac{-E_a}{RT}\right) \qquad (1)$$

On anode ‘A’, the value of α is 0.85 ± 0.05. On anode ‘B’, a much higher dependency on methane partial pressure is observed: 1.4 ± 0.01. This is close to

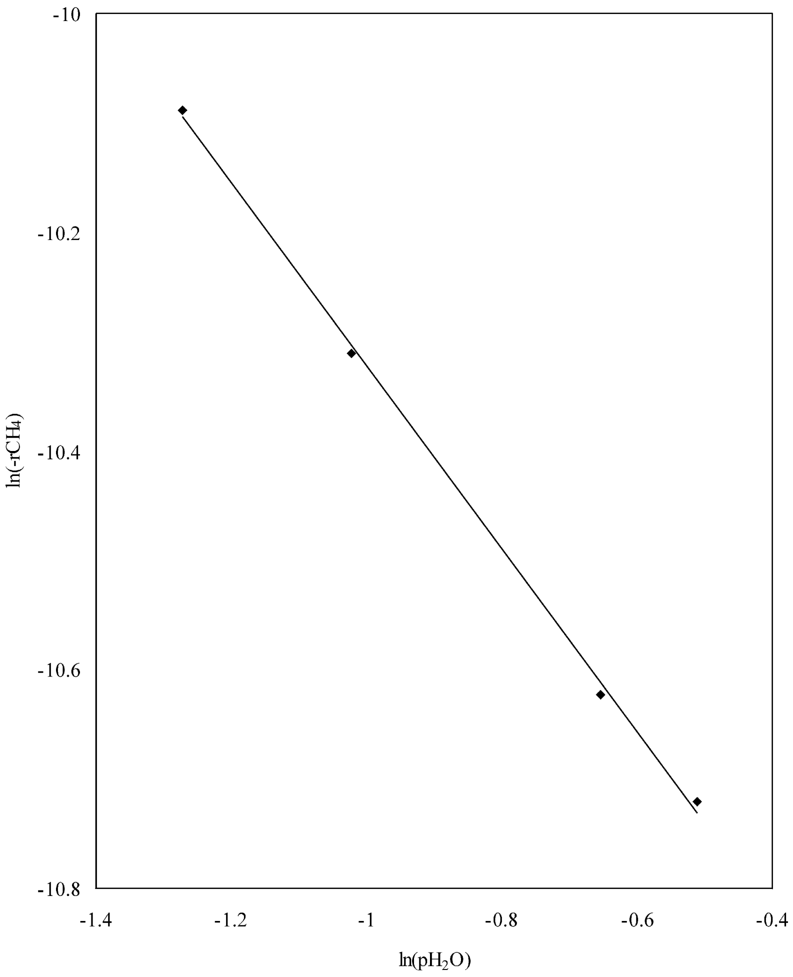

Fig. 4. Rate of reforming vs. p_{H_2O} on anode ‘B’ (895°C, S/C = 1.4 to 3.0, $p_{CH_4} = 0.2$ bar).

the value of 1.2 reported by Odegaard et al. [4] on a Ni–ZrO_2 anode. Most researchers, however, have reported first-order kinetics with respect to methane. The results of our study are shown in Figs. 1 and 2.

On anode ‘A’, a slightly negative order dependency with respect to steam was obtained with a value of -0.35 ± 0.04 for β. On anode ‘B’, increased negative order dependency was observed with a value of -0.8 ± 0.02. Figs. 3 and 4 show the order dependency in steam for the two anodes.

In order to open up the operational window for steam reforming over a wider range of S/C ratios, steam reforming catalysts are modified by the addition of basic compounds, e.g. alkali and alkaline earth metals, for suppression of carbon formation by improving steam retention [12]. This approach proved effective also for SOFC anodes as demonstrated by Singh et al. [13] who reported reduced carbon deposition tendencies during internal steam reforming when the nickel–zirconia cermet anode was modified by impregnation with salts of Mg, Ca, Al, Sr, Ce and Ba followed by calcination to form the appropriate oxides. However, modifications of this type, in general, result in lower reforming rates and increased negative reaction orders with respect to steam. Dicks et al. [11] reported negative steam partial pressure dependencies

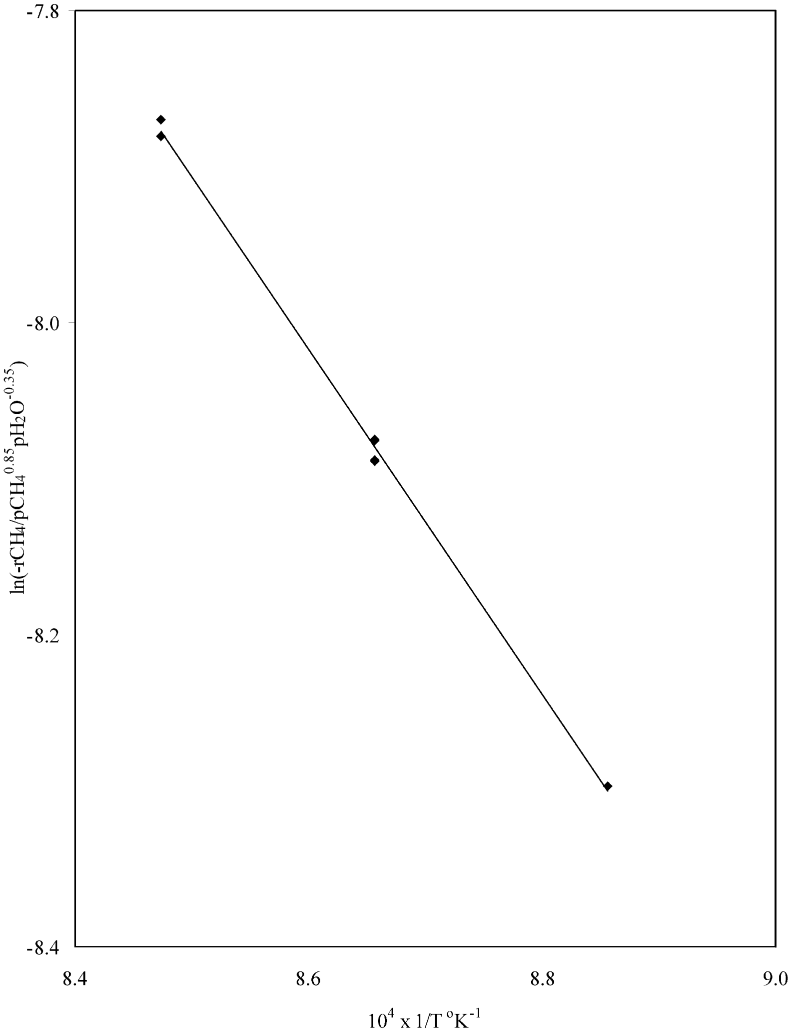

Fig. 5. Arrhenius plot of reforming on anode 'A' (854–907°C, S/C = 1.5 to 3.0, $p_{CH_4} = 0.15$ to 0.3 bar, $p_{H_2O} = 0.23$ to 0.45 bar).

of −0.4 at 900°C and −0.8 at 800°C. Only Zhuang et al. [14] found low coking tendencies as well as higher steam reforming rates for ceria doped Ni/MgAl$_2$O$_4$ catalysts.

Several rate expressions based on various kinetic models have been proposed in the literature [15–17] to explain experimental observations. Of these, the most comprehensive treatment was put forward by Xu and Froment [17] who proposed the following rate expression for the reaction of methane and steam to carbon monoxide and hydrogen.

$$r = \frac{(k/p_{H_2}^{2.5})(p_{CH_4}p_{H_2O} - p_{CO}p_{H_2}^{3}/k_{eq})}{(1 + k_{CO}p_{CO} + k_{H_2}p_{H_2} + k_{CH_4}p_{CH_4} + k_{H_2O}p_{H_2O}/p_{H_2})^2} \qquad (2)$$

This form of rate expression explains the negative order in steam observed in our experiments.

Activation energy on anode 'A' was 95 ± 2 kJ/mol which is similar to the values reported on Ni–ZrO$_2$ anodes [3,4]. On anode 'B' the reforming rates were much lower with an activation energy of 208 ± 10 kJ/mol. This is similar to that reported on

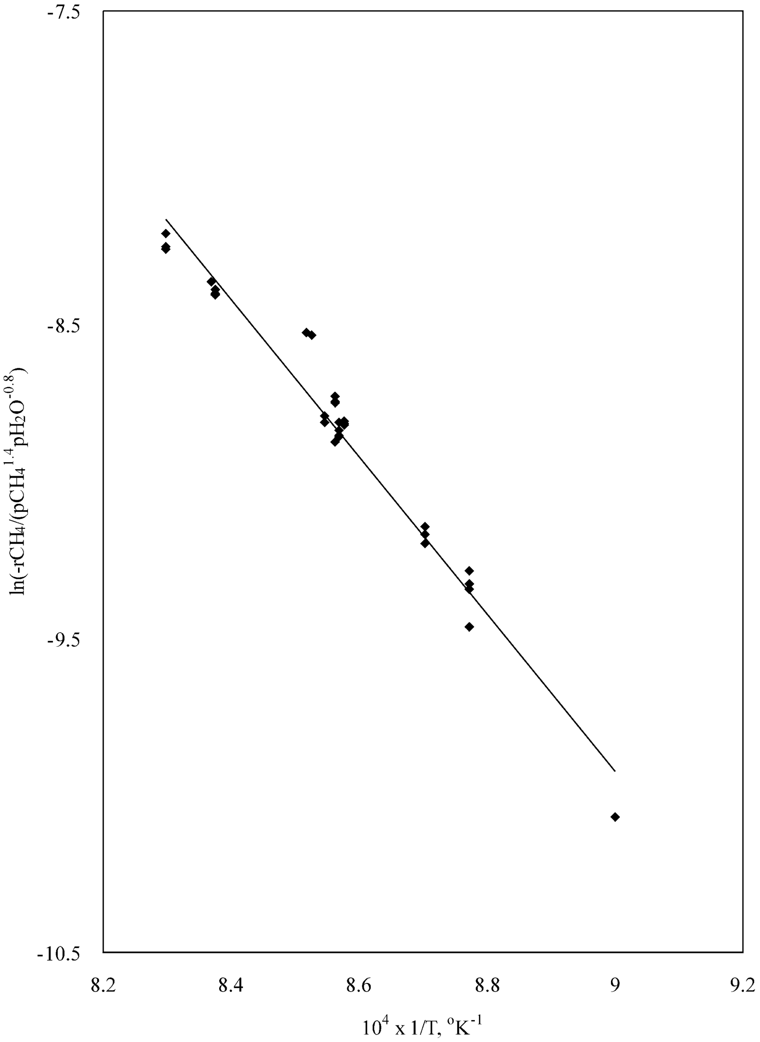

Fig. 6. Arrhenius plot of reforming on anode 'B' (838–922°C, S/C = 1.4 to 3.0, $p_{CH_4} = 0.2$ to 0.35 bar, $p_{H_2O} = 0.28$ to 0.60 bar).

a Ni–ZrO_2–CeO_2 anode [6]. The Arrhenius plots from our study are shown in Figs. 5 and 6. The value of the pre-exponential factor was higher on Anode 'B', being 3.6E8 mol/s m^2 $bar^{0.6}$ compared to 8542 mol/s m^2 $bar^{0.5}$ on Anode 'A'.

High activation energies have been reported. Dicks et al. [11] reported non-linearity of Arrhenius plots with composition dependent activation energies of 118–294 kJ/mol. Belyaev et al. [6] who studied the kinetics of steam reforming on a Ni–ZrO_2–CeO_2 anode found low reforming rates and reported an activation energy of 163 kJ/mol which was much higher than the values of 58 and 82 kJ/mol on Ni–ZrO_2 anodes reported by Odegaard et al. [4] and Achenbach and Riensche [3], respectively. Divisek et al. [10] reported an even higher activation energy of 230 kJ/mol.

The large difference in the values of the pre-exponential factor and the activation energy for the two anodes in our study suggests that both the number and the nature of sites has changed by incorporation of the basic compound into the catalyst. We propose that the active sites responsible for reforming activity and carbon formation resistivity in Anode 'B' involve both the nickel and the additive. Reforming activity on the additive alone may be a few orders of magnitude lower than on nickel. This would explain the higher activation energy and hence the lower rate of reforming on anode 'B'. The reaction of methane and steam may involve the following sequence of steps:

$$CH_4 = CH_{2ads} + H_2 \tag{3}$$

$$CH_{2ads} = C_{ads} + H_2 \tag{4}$$

$$C_{ads} + H_2O = CO + H_2O \tag{5}$$

$$CO + H_2O = CO_2 + H_2 \tag{6}$$

The rate determining steps in the above sequence may be (3) or (4) or (5). If the nature of sites is different in the two catalysts, the rate-limiting steps may also be different resulting in different order dependencies of the reactants, different pre-exponential factors and different activation energies.

4. Conclusions

Kinetics of methane steam reforming on Ni–ZrO_2 anodes is significantly affected by the addition of certain basic compounds to the anode composition. In our study, we found the reaction order in methane increased from 0.85 for a Ni–ZrO_2 anode to 1.4 for a modified Ni–ZrO_2 anode. Similarly, the dependency on steam increased from -0.35 to -0.8. Activation energy for the modified anode was much higher being ca. 210 kJ/mol compared to ca. 95 kJ/mol for the Ni–ZrO_2 anode indicating a much lower reforming rate on the modified anode. We propose that both the number and the nature of active sites are changed by incorporation of the basic compound in the Ni/YSZ anode formulation. As a result, the rate-limiting step in a proposed reaction sequence may be different on the two catalysts so that the activation energy, pre-exponential factor and partial pressure dependencies of reactants are different.

References

[1] K. Ahmed, P. Seshadri, Y. Ramprakash, S.P. Jiang, K. Foger, in: U. Stimmung, S.C. Singhal, H. Tagawa, W. Lehnert (Eds.), Proceedings of the Fifth International Symposium on SOFCs, The Electrochemical Society, 1997, p. 228.
[2] J. Parsons, S. Randall, SOFC-micromodelling IEA-SOFC-Task Report, Berne, May 1992, p. 43.
[3] E. Achenbach, E. Riensche, J. Power Sources 52 (1994) 283.
[4] R. Odegaard, E. Johnsen, H. Karoliussen, in: M. Dokiya, O. Yamamoto, H. Tagawa, S.C. Singhal (Eds.), Proceedings of the Fourth International Symposium on SOFCs, The Electrochemical Society, 1995, p. 810.
[5] K. Eguchi, M. Kayano, Y. Kunisa, H. Arai, in: M. Dokiya, O. Yamamoto, H. Tagawa, S.C. Singhal (Eds.), Proceedings of the Fourth International Symposium on SOFCs, The Electrochemical Society, 1995, p. 676.
[6] V.D. Belyaev, T.I. Politova, O.A. Marina, V.A. Sobyanin, Appl. Catal. A 133 (1995) 47.
[7] I.V. Yentekakis, S.G. Neophytides, A.C. Kaloyiannis, C.G. Vayenas, in: S.C. Singhal, H. Iwahara (Eds.), Proceedings of the Third International Symposium on SOFCs, The Electrochemical Society, 1993, p. 904.
[8] S. Bebelis, S. Neophytides, C. Vayenas, in: U. Bossel (Ed.), Proceedings of the First European SOFC Forum, The European SOFC Forum Secretariat, 1994, p. 197.
[9] A.L. Lee, R.F. Zabransky, W.J. Huber, Ind. Eng. Chem. Res. 29 (1990) 766.
[10] J. Divisek, W. Lehnert, J. Meusinger, U. Stimming, in: U. Stimming, S.C. Singhal, H. Tagawa, W. Lehnert (Eds.), Proceedings of the Fifth International Symposium on SOFCs, The Electrochemical Society, 1997, p. 993.
[11] A.L. Dicks, K.D. Pointon, A. Swann, in: P. Stevens (Ed.), Proceedings of the Third European SOFC Forum, The European SOFC Forum Secretariat, 1998, p. 249.
[12] J.R. Rostrup-Nielsen, Catalytic steam reforming, in: J.R. Anderson, M. Boudart (Eds.), Catalysis Science and Technology, Vol. 5, Springer, Berlin, 1984, p. 1.
[13] P. Singh, R.J. Ruka, R.A. George, US Patent 4,894,297 (1990), Westinghouse Electric Corporation.
[14] Q. Zhuang, Y. Qin, L. Chang, Appl. Catal. A 70 (1991) 1.
[15] I.M. Bodrov, L.O. Apel'baum, M.I. Temkin, Kinet. Katal. 5 (1964) 696.
[16] A.A. Khomenko, L.O. Apel'baum, F.S. Shub, Y.S. Snagovskii, M.I. Temkin, Kinet. Katal. 12 (1971) 423.
[17] J. Xu, G.F. Froment, AIChE J. 35 (1989) 88.